sciendo

Modeling of transport properties of binary mixtures including ionic liquids based on their experimental estimation

Pavol Steltenpohl, Anna Holečková, Elena Graczová

Institute of Chemical and Environmental Engineering, Faculty of Chemical and Food Technology, Slovak University of Technology in Bratislava, Radlinského 9, 812 37 Bratislava, Slovak Republic
pavol.steltenpohl@stuba.sk

Abstract: Transport properties of selected imidazolium ionic liquids (1-ethyl-3-methylimidazolium acetate, [emim][ac], and 1-butyl-3-methylimidazolium trifluoromethanesulfonate, [bmim][triflate]) as well as of binary mixtures of these ILs with water and ethanol were estimated experimentally. Density data were obtained within the temperature range of 293.15—333.15 K and used for the excess molar volume calculations. For the binary mixtures comprising selected ionic liquids and water/ethanol, partial molar volumes of mixture components were computed and the excess molar volume variation with the mixture composition was correlated using the Redlich-Kister equation. Dependence of viscosity on the binary mixture composition and temperature was described using the Jouyban-Acree model. These data form a base for the assessment of OPEX connected with transportation of mixtures containing these ionic liquids.

Keywords: imidazolium ionic liquids, density, dynamic viscosity, transportation expenses

Introduction

Negative impact of volatile organic solvents used in chemical technology on the environment and human health is very well known and documented (see e.g. Li et al. (2021)). New alternatives replacing these traditional solvents include, among others, ionic liquids (ILs). This type of salts possesses specific and very interesting properties (Welton, 1999; Hallett & Welton, 2011). They are liquid already at room or slightly elevated temperatures but they show negligible vapor pressure within the range of their typical operation temperatures. Properties of this class of compounds can be finely adjusted by modifying their anion or cation (Nieto de Castro et al., 2010; Eyckens & Henderson, 2019). In this way, their selectivity and capacity in separation processes, as well as their transport properties (density and viscosity) or catalytic activity can be set-up.

Due to their nature, ILs found use in diverse fields of (chemical) industry and numerous processes (Steltenpohl & Graczová, 2022). Recently, a comprehensive review of the areas of ILs application was published by Kaur et al. (2022). ILs take part in such different processes as electrochemistry, separation, organic synthesis, and enzymatic reactions, in food, pharmaceutical, and biochemical industry, in analytical chemistry, as an additive or in environmental protection (Kaur et al., 2022).

In this paper, transport properties, namely density and viscosity, of two imidazolium ionic liquids, 1-ethyl-3-methylimidazolium acetate ([emim][ac]) and 1-butyl-3-methylimidazolium trifluoromethanesulfonate ([bmim][triflate]), and their mixtures with water or ethanol were estimated within the temperature range of 20—60 °C. To the best of our knowledge, no experimental viscosity data have been published for the binary system [bmim][triflate]—ethanol. Obtained experimental data were processed with the aim to predict their dependence on the binary mixture composition. In case of the density measurement, excess molar volume of the prepared binary mixtures was computed and its variation with the IL content in the mixture was correlated using the Redlich-Kister equation (Redlich & Kister, 1948). Regarding viscosity data, variation of this parameter with the mixture composition and temperature was described using the Jouyban-Acree model (Acree, 1992).

Theoretical

Densities of the binary mixtures of studied ionic liquids with water and ethanol were used to calculate the excess molar volumes, V^{E}, and the mixture components' partial molar volumes, $\bar{V}_i$. Variation of the excess molar volume with the mixture composition was correlated using the Redlich-Kister equation.

Equation defining the above-mentioned variables can be found, e.g., in Steltenpohl & Graczová (2022). The Redlich-Kister equation correlating the excess molar volume variation with the mixture composition is given as follows (Redlich & Kister, 1948):

$$V^{\mathrm{E}} = x_1 x_2 \sum_n C_n \left(x_1 - x_2\right)^{n-1} \tag{1}$$

Tab. 1. Basic data of chemicals used.

Component	CAS	M/(kg · mol^{-1})	Declared purity	Water content
[emim][ac]	143314-17-4	0.17021	> 98.0 %	0.512 %
[bmim][triflate]	174899-66-2	0.28829	> 99.0 %	239 ppm
water	7732-18-5	0.01802	de-ionized	–
ethanol	64-17-5	0.04607	> 99.9 %	221 ppm

where x_1, x_2 are the mixture components' mole fractions, C_n represent the model parameters and $n - 1$ is the polynomial order.

Partial molar volumes of the mixture components were expressed according to Wood & Battino (1990):

$$\overline{V}_i = V^{\mathrm{E}} + V_i^* + (1 - x_i)\left(\frac{\partial V^{\mathrm{E}}}{\partial x_i}\right)_{P,T} \qquad i = 1, 2 \tag{2}$$

here V_i^* denotes molar volume of component i, and the term representing variation of the excess molar volume with the mixture composition, $(\partial V^{\mathrm{E}}/\partial x_i)_{p,T}$, was derived by differentiating the Redlich-Kister equation (Eq. 1). Symbols P and T correspond to the system pressure and temperature, respectively.

Optimum values of model parameters given in Eq. 1 were obtained by minimizing the objective function, OF, in the following form:

$$OF = \sum_N \left(V^{\mathrm{E}}_{\mathrm{exp},j} - V^{\mathrm{E}}_{\mathrm{calc},j}\right)^2 = \min \tag{3}$$

where N is the number of experimental points.

Standard residual deviations of experimental data, $\sigma_{V^{\mathrm{E}}}$, were calculated based on their definition.

Variation of the binary mixture viscosity, η, with its temperature and composition was described applying the Jouyban-Acree equation (Acree, 1992):

$$\ln \eta_{\mathrm{exp},T} = \sum_i x_i \ln \eta_{i,T} + x_1 x_2 \sum_n J_n \frac{(x_1 - x_2)^{n-1}}{T} \tag{4}$$

where subscript exp corresponds to the experimental (measured) value, and J_n stand for the model parameters.

For the estimation of optimum parameters of the Jouyban-Acree model equation, the following objective function was applied:

$$OF = \sum_N \left(\frac{\eta_{\mathrm{exp},j} - \eta_{\mathrm{calc},j}}{\eta_{\mathrm{exp},j}}\right)^2 = \min \tag{5}$$

For comparison of the quality of experimental viscosity data, the relative root mean square error values were computed.

Experimental

Ionic liquids used in this study were supplied by Iolitec (purity above 98 %). De-ionized water was used for the preparation of binary mixtures IL (1)—water (2). Absolute ethanol (above 99.9 %) was purchased from Slavus, Bratislava. Basic data of all chemicals used in this study as well as declared and estimated water content in ILs and in ethanol are given in Table 1.

Samples of the supplied ionic liquids were used without purification. Water content in the ILs and ethanol was checked using a Karl Fischer titrator (Mettler Toledo DL53) and the results of this measurement are included in Table 1.

IL (1)—water/ethanol (2) binary mixtures were obtained by precisely weighing the mixture components using Mettler AE 200 analytical balance. Accuracy of the mass reading was $\pm 1 \times 10^{-4}$ g.

Density of the samples containing ionic liquids at ambient pressure was measured using Anton Paar Densimeter DMA 5000. Declared standard uncertainty of density measurements using this equipment was $\pm 2 \times 10^{-2}$ kg · m^{-3}. Density values of the samples were determined at three temperatures, namely 20 °C, 40 °C and 60 °C. Accuracy of temperature readings was $\pm 1 \times 10^{-3}$ °C.

A Malvern Kinexus parallel plate rheometer was used to measure the binary mixtures' viscosity. Experimental data were obtained at the temperatures of 20 °C, 40 °C and 60 °C. Accuracy of the set-up temperatures measurement was $\pm 1 \times 10^{-2}$ °C.

Results and discussion

In Table 2, experimental and literature values of pure components' densities at chosen temperatures are summarized. Data for pure components viscosities are given in Table 3.

Computed values of the excess molar volume and the components partial molar volume for the four binary systems of interest, i.e. [emim][ac] (1)—water (2), [bmim][triflate] (1)—water (2), [emim][ac] (1)—ethanol (2) and [bmim][triflate] (1)—ethanol (2), are shown in Tables 4—7, respectively.

Data presented in Table 2 were fitted using a third-order Redlich-Kister equation (Eq. 1). Model parameters were obtained via minimization of the objective function given by Eq. 3 and are collected in Table 8. This procedure was applied to all binaries of interest and for all experimental temperature values. Table 8 also includes the values

Tab. 2. Experimental and literature density of components at chosen temperatures.

Component	Density, ρ/(kg · m^{-3})						Source
	Experimental			Literature			
	20 °C	40 °C	60 °C	20 °C	40 °C	60 °C	
[emim][ac]	1090.7	1078.3	1066.0	1103.0	1091.0	1079.0	Zhang et al. (2017)
[bmim][triflate]	1302.8	1287.0	1271.4	1303.5	1287.7	1272.1	Tariq et al. (2009)
water	998.24	992.23	982.67	998.21	992.22	983.20	NIST (2021)
ethanol	792.50	775.19	756.96	789.45	772.44	754.30	NIST (2021)

Tab. 3. Experimental and literature viscosity of components at chosen temperatures.

Component	Dynamic viscosity, η/(mPa · s)						Source
	Experimental			Literature			
	20 °C	40 °C	60 °C	20 °C	40 °C	60 °C	
[emim][ac]	111.1	32.5	14.1	179.1	60.4	26.7	Zhang et al. (2017)
[bmim][triflate]	117.2	47.3	23.4	128.5	51.3	25.5	Tariq et al. (2009)
water	1.001	–	–	1.002	0.653	0.466	NIST (2021)
ethanol	1.139	–	–	1.144	0.794	0.570	NIST (2021)

Tab. 4. Excess molar volume of the binary system [emim][ac] (1)—water (2), and component partial molar volumes at 20 °C, 40 °C and 60 °C.

Sample	Composition		V^E/(cm^3 · mol^{-1})			$\bar{V}_1$/(cm^3 · mol^{-1})			$\bar{V}_2$/(cm^3 · mol^{-1})		
	x_1	x_2	20 °C	40 °C	60 °C	20 °C	40 °C	60 °C	20 °C	40 °C	60 °C
1	0.0977	0.9023	–0.7708	–0.6731	–0.5987	149.49	151.77	154.00	17.16	17.70	18.15
2	0.1958	0.8042	–1.3005	–1.1932	–1.1058	152.13	153.92	155.76	16.45	17.04	17.56
3	0.2880	0.7120	–1.4620	–1.3785	–1.3104	153.90	155.57	157.29	16.01	16.48	16.95
4	0.3835	0.6165	–1.4477	–1.3881	–1.3421	155.08	156.79	158.50	15.76	16.09	16.46
5	0.4777	0.5223	–1.3241	–1.2822	–1.2530	155.73	157.49	159.25	15.70	15.92	16.20
6	0.5518	0.4482	–1.1740	–1.1422	–1.1245	155.98	157.77	159.57	15.74	15.92	16.14
7	0.6284	0.3716	–1.0001	–0.9737	–0.9592	156.08	157.86	159.69	15.81	15.99	16.17
8	0.6946	0.3054	–0.7769	–0.7575	–0.7388	156.08	157.86	159.71	15.86	16.04	16.23

Tab. 5. Excess molar volume of the binary system [bmim][triflate] (1)—water (2), and component partial molar volumes at 20 °C, 40 °C and 60 °C.

Sample	Composition		V^E/(cm^3 · mol^{-1})			$\bar{V}_1$/(cm^3 · mol^{-1})			$\bar{V}_2$/(cm^3 · mol^{-1})		
	x_1	x_2	20 °C	40 °C	60 °C	20 °C	40 °C	60 °C	20 °C	40 °C	60 °C
1	0.1045	0.8955	–0.0932	0.0291	0.1442	221.19	224.64	228.10	17.22	17.63	18.06
2	0.2015	0.7985	–0.0697	0.0857	0.2334	221.72	224.74	227.79	17.33	17.81	18.31
3	0.3005	0.6995	–0.0131	0.1464	0.2982	221.61	224.44	227.29	17.70	18.14	18.64
4	0.3905	0.6095	0.0154	0.1653	0.3074	221.41	224.17	226.96	17.97	18.37	18.81
5	0.4984	0.5016	0.0351	0.1653	0.2869	221.30	224.04	226.80	18.09	18.43	18.82
6	0.5925	0.4075	0.0564	0.1663	0.2668	221.35	224.08	226.85	18.04	18.37	18.73
7	0.6967	0.3033	0.0428	0.1254	0.1993	221.46	224.19	226.95	18.02	18.35	18.71
8	0.7902	0.2098	0.0710	0.1260	0.1789	221.49	224.21	226.97	18.25	18.59	18.98
9	0.8911	0.1089	0.1640	0.1981	0.2307	221.40	224.11	226.87	19.03	19.39	19.80

Tab. 6. Excess molar volume of the binary system [emim][ac] (1)—ethanol (2), and component partial molar volumes at 20 °C, 40 °C and 60 °C.

Sample	Composition		$V^E/(cm^3 \cdot mol^{-1})$			$\bar{V}_1/(cm^3 \cdot mol^{-1})$			$\bar{V}_2/(cm^3 \cdot mol^{-1})$		
	x_1	x_2	20 °C	40 °C	60 °C	20 °C	40 °C	60 °C	20 °C	40 °C	60 °C
1	0.1001	0.8999	–0.4876	–0.5912	–0.7717	150.96	152.01	152.68	57.30	58.36	59.32
2	0.1994	0.8006	–0.5923	–0.7295	–0.9555	153.14	154.60	155.98	56.67	57.64	58.49
3	0.3000	0.7000	–0.7344	–0.8816	–1.1191	154.61	156.28	157.95	56.32	57.28	58.19
4	0.3980	0.6020	–0.3190	–0.4415	–0.6519	155.51	157.28	159.04	56.22	57.21	58.22
5	0.4982	0.5018	–0.0875	–0.1863	–0.3674	155.99	157.79	159.57	56.47	57.50	58.58
6	0.5805	0.4195	0.2481	0.1782	0.0307	156.07	157.88	159.67	57.02	58.09	59.21
7	0.6588	0.3412	0.4649	0.4199	0.3023	155.92	157.72	159.53	57.95	59.06	60.19
8	0.7395	0.2605	0.9637	1.0722	0.7996	155.56	157.34	159.17	59.42	60.58	61.72
9	0.7977	0.2023	0.8412	0.8326	0.7719	155.21	156.99	158.81	60.86	62.07	63.23

Tab. 7. Excess molar volume of the binary system [bmim][triflate] (1)—ethanol (2), and component partial molar volumes at 20 °C, 40 °C and 60 °C.

Sample	Composition		$V^E/(cm^3 \cdot mol^{-1})$			$\bar{V}_1/(cm^3 \cdot mol^{-1})$			$\bar{V}_2/(cm^3 \cdot mol^{-1})$		
	x_1	x_2	20 °C	40 °C	60 °C	20 °C	40 °C	60 °C	20 °C	40 °C	60 °C
1	0.0962	0.9038	–0.5763	–0.6402	–0.7617	218.13	220.36	222.15	56.98	58.29	60.00
2	0.2008	0.7992	–0.5988	–0.6803	–0.8281	220.30	222.73	224.80	56.64	57.84	59.26
3	0.3050	0.6950	–0.5348	–0.6178	–0.7670	221.13	223.78	226.41	56.83	57.92	58.95
4	0.3955	0.6045	–0.5054	–0.5845	–0.7266	221.37	224.15	227.14	57.09	58.13	58.99
5	0.4958	0.5042	–0.5544	–0.6271	–0.7576	221.46	224.30	227.42	57.33	58.39	59.29
6	0.6012	0.3988	–0.3647	–0.4208	–0.5270	221.52	224.33	227.35	57.49	58.64	59.82
7	0.6993	0.3007	–0.0346	0.0287	0.2794	221.54	224.30	227.14	57.66	58.91	60.39
8	0.8018	0.1982	0.0730	0.0541	0.0068	221.50	224.21	226.92	58.05	59.36	60.98
9	0.9019	0.0981	–0.0854	–0.0959	–0.1250	221.37	224.08	226.78	58.84	60.11	61.46

Tab. 8. Summary of excess molar volume correlations: optimum values of the third-order Redlich-Kister model parameters and computed standard residual deviations.

Parameter	t/°C	Binary system			
		[emim][ac]—H_2O	[bmim][triflate]—H_2O	[emim][ac]—EtOH	[bmim][triflate]—EtOH
C_1	20	–5.1522	0.1143	–0.2861	–1.6750
	40	–4.9989	0.6264	–0.6649	–1.8875
	60	–4.9040	1.1028	–1.3846	–2.1844
C_2	20	4.2175	–0.0471	7.6464	2.4202
	40	3.9729	–0.4634	8.5124	3.0945
	60	3.7134	–0.8940	8.8463	4.8747
C_3	20	–1.3119	0.0447	3.0343	–1.0860
	40	–0.7841	0.4825	3.2512	–1.2147
	60	–0.1134	0.9173	2.0587	–1.5312
C_4	20	–0.6711	2.6438	1.4711	2.1870
	40	–1.4712	2.3329	1.7424	1.6321
	60	–1.6782	2.1217	2.2812	–0.4566
$\sigma_{V^E}/(cm^3 \cdot mol^{-1})$	20	0.0255	0.0252	0.1121	0.1321
	40	0.0254	0.0285	0.1515	0.1572
	60	0.0259	0.0311	0.1023	0.2544

of standard residual deviations of the excess molar volumes, σ_{V^E}.

Comparison of experimental and computed values of excess molar volume are shown in Figs. 1–4 for the four investigated binary mixtures, namely [emim][ac] (1)–water (2), [bmim][triflate] (1)–water (2), [emim][ac] (1)–ethanol (2) and [bmim][triflate] (1)–ethanol (2).

Relatively symmetric parable with a minimum of the excess molar volume at the [emim][ac] molar fraction of about 0.35 is observed for the binary system [emim][ac] (1)–water (2) in Fig. 1. With the temperature increase, the minimum in excess molar volume vs. composition curve is shifted to higher IL content, from 0.33 at 20 °C to 0.38 at 60 °C. Presented results confirm that the temperature effect is more noticeable in the region of higher water content (Bahadur et al., 2015). Also, the measured and computed V^E values increased with the temperature.

In Fig. 2, a very complex, although not unique (Bahadur et al., 2015), behavior is observed in the course of the excess molar volume variation with the mixture composition for the binary system [bmim][triflate] (1)–water (2). There are two maxima and a minimum of V^E in the measured data and computed curves. The minimum in computed data appears close to the pure water pole. The two maxima are located at the IL mole fractions of 0.35 and 0.85. The effect of temperature on the mixture excess molar volume is large as shown by the significantly diverging courses of the three curves presented.

In case of the [emim][ac] (1)–ethanol (2) mixture, a relatively symmetric sinusoidal course of V^E variation with x_1 is observed (Fig. 3). The minimum of these curves is located close to 30 mole % while the maximum is found at about 80 mole % of IL in the binary mixture. It seems that the increase of temperature has a negative effect on the excess molar volume.

Sinusoidal shape of the excess molar volume variation with the mixture composition is also found in Fig. 4. The picture is quite similar to that observed in Fig. 3; however, it is less symmetric with respect to the central line of $V_E = 0$. Quality of the fit was severely affected by the dispersion of the measured data as shown by the values of computed standard residual deviations for the binary system [bmim][triflate] (1)–ethanol (2) (see Table 8).

Experimental viscosity values of the four binary systems of interest were correlated using the Jouyban-Acree model (Eq. 4) for the whole region of temperatures. The Jouyban-Acree model parameters were obtained by minimizing the squared relative differences of experimental and computed viscosity values (Eq. 5) and are summarized in Table 9 together with the values of standard residual deviations. The polynomial order $n - 1 = 3$ was chosen when fitting the experimental viscosity data.

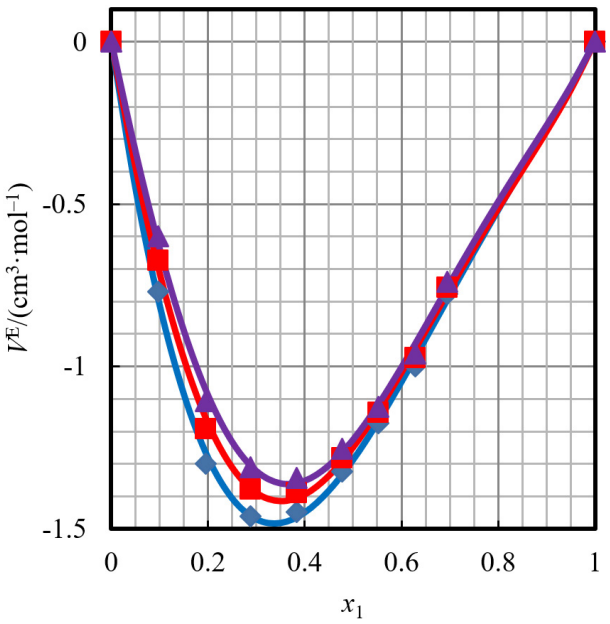


Fig. 1. Variation of excess molar volume of the binary mixture [emim][ac] (1)–water (2) with the mixture composition at 20 °C (blue color), 40 °C (red color), and 60 °C (violet color). Symbols represent experimental and curves computed data.

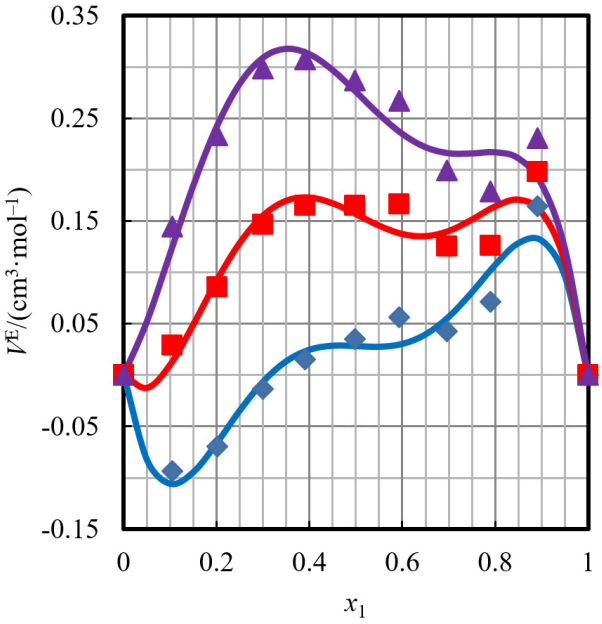


Fig. 2. Variation of excess molar volume of the binary mixture [bmim][triflate] (1)–water (2) with the mixture composition at 20 °C (blue color), 40 °C (red color), and 60 °C (violet color). Symbols represent experimental and curves computed data.

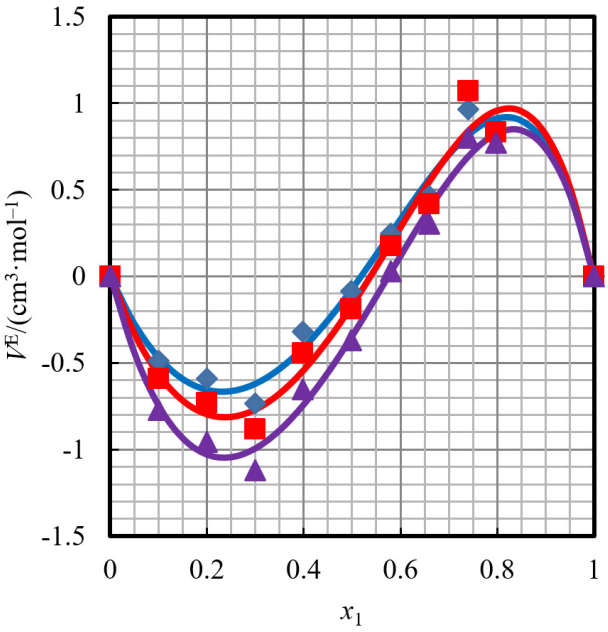


Fig. 3. Variation of excess molar volume of the binary mixture [emim][ac] (1)—ethanol (2) with the mixture composition at 20 °C (blue color), 40 °C (red color), and 60 °C (violet color). Symbols represent experimental and curves computed data.

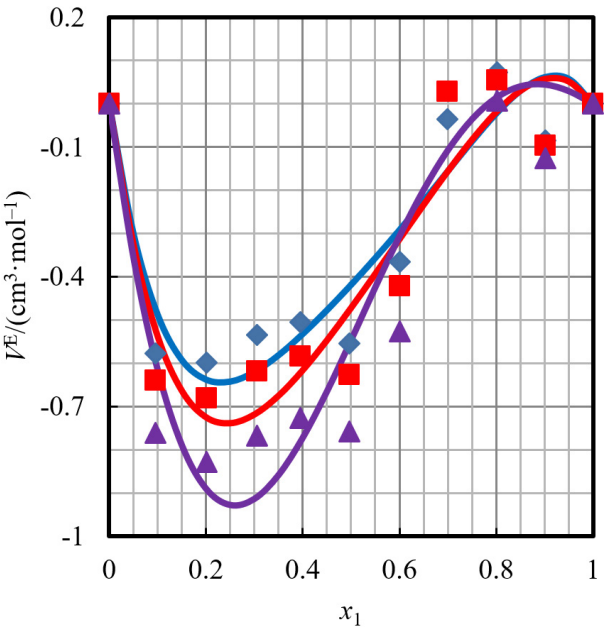


Fig. 4. Variation of excess molar volume of the binary mixture [bmim][triflate] (1)—ethanol (2) with the mixture composition at 20 °C (blue color), 40 °C (red color), and 60 °C (violet color). Symbols represent experimental and curves computed data.

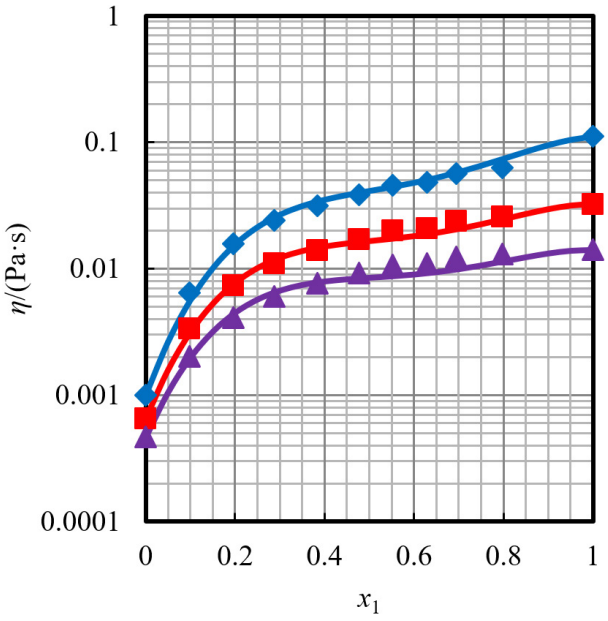


Fig. 5. Variation of viscosity of the binary mixture [emim][ac] (1)—water (2) with the mixture composition at 20 °C (blue color), 40 °C (red color), and 60 °C (violet color). Symbols represent experimental and curves computed data.

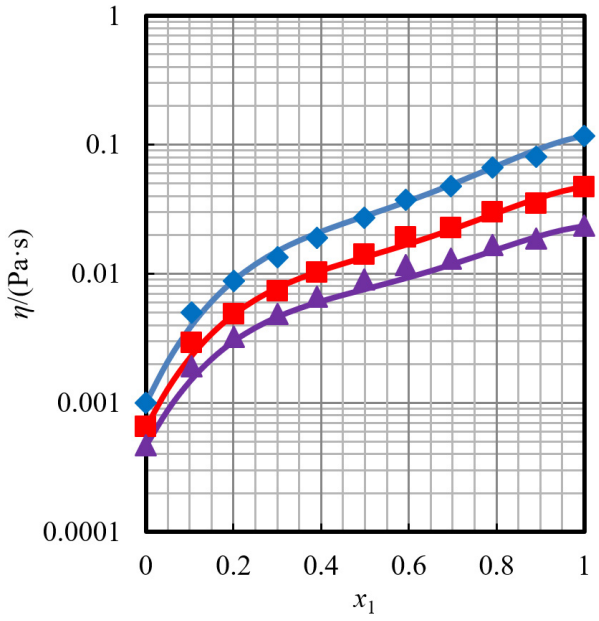


Fig. 6. Variation of viscosity of the binary mixture [bmim][triflate] (1)—water (2) with the mixture composition at 20 °C (blue color), 40 °C (red color), and 60 °C (violet color). Symbols represent experimental and curves computed data.

In Figs. 5—8, variation of viscosity with the binary mixture composition is shown for the chosen binary systems [emim][ac] (1)—water (2), [bmim][triflate] (1)—water (2), [emim][ac] (1)—ethanol (2) and [bmim][triflate] (1)—ethanol (2), respectively. Experimental data were compared with the curves computed using the Jouyban-Acree model equation.

Tab. 9. Summary of the viscosity difference correlation: optimum values of the Jouyban-Acree model and computed relative root mean square error values.

Parameter	Binary system			
	[emim][ac]–H_2O	[bmim][triflate]–H_2O	[emim][ac]–EtOH	[bmim][triflate]–EtOH
J_1	1598.80	1100.61	498.77	628.73
J_2	–1930.56	–1263.26	–544.79	–252.40
J_3	1523.28	1124.38	38.66	–32.00
RRMSE/%	2.15	1.66	1.60	1.17

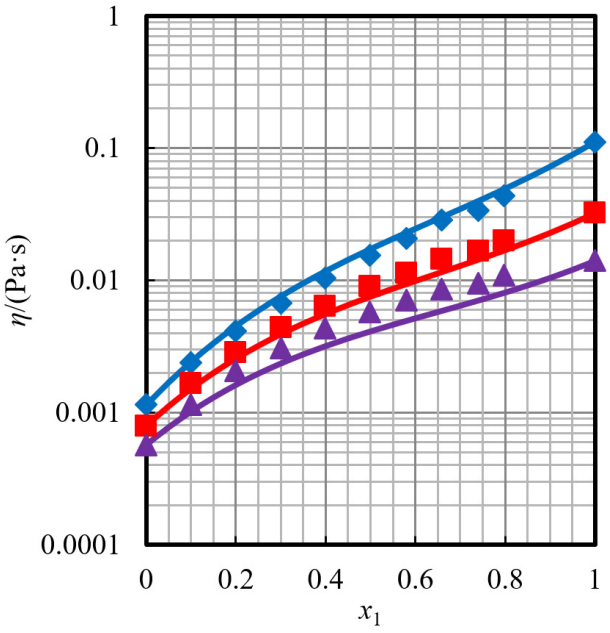


Fig. 7. Variation of viscosity of the binary mixture [emim][ac] (1)–ethanol (2) with the mixture composition at 20 °C (blue color), 40 °C (red color), and 60 °C (violet color). Symbols represent experimental and curves computed data.

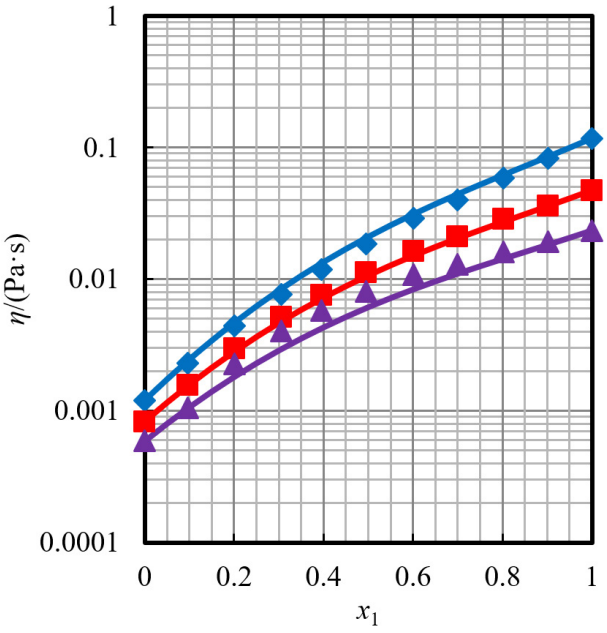


Fig. 8. Variation of viscosity of the binary mixture [bmim][triflate] (1)–ethanol (2) with the mixture composition at 20 °C (blue color), 40 °C (red color), and 60 °C (violet color). Symbols represent experimental and curves computed data.

A close fit of the experimental data was obtained for all binary systems of interest as shown in Figs. 5–8. Slightly better correlation of experimental data was obtained for the mixtures containing ethanol compared to the respective aqueous mixtures as also displayed by the values of relative root mean square error summarized in Table 9.

Conclusions

Density and viscosity of four binary mixtures containing [emim][ac] and [bmim][triflate] ionic liquids and water or ethanol were measured at the temperatures of 20 °C, 40 °C, and 60 °C within the entire concentration range. The sets of experimental density values were used to compute excess molar volume and component partial molar volume for the individual binary mixtures at isothermal conditions. Variation of these parameters with the mixture composition was correlated using the third-order Redlich-Kister equation.

Computed values of the average standard deviation of the excess molar volume oscillated around the value of 0.02 $cm^3 \cdot mol^{-1}$ for binary mixtures containing water (Table 8). Slightly worse goodness of fit of the excess molar volume correlation was observed in case of binaries comprising ethanol, where the values of standard deviation exceeded 0.1 $cm^3 \cdot mol^{-1}$ (Table 8). Very complex behavior, excess molar variation with the mixture composition, was observed for the binary mixture [bmim][triflate]–water (Fig. 2).

In case of viscosity measurements, non-isothermal data sets of the four binary systems were fitted using the Jouyban-Acree model. Correlation of the experimental viscosities was successful with the relative root mean square error of 1.1–2.2 % (Table 9). Slightly less accurate description of the

experimental data was obtained for the binary systems comprising water compared to those containing ethanol. Separately calculated values of the standard residual deviation ranged between 2—4 mPa · s.

This study was presented at the 48th International Conference of the Slovak Society of Chemical Engineering (May 18—19, 2022, Tatranské Matliare, Slovakia).

Acknowledgement
Financial support of the Slovak Research and Development Agency under the contract No. APVV-0232-18 is acknowledged.

References

Acree WE Jr. (1992) Thermochim. Acta 198: 71—79.
Bahadur I, Letcher TM, Singh S, Redhi GG, Venkatesu P, Ramjugernath D (2015) J. Chem. Thermodyn. 82: 34—46.
Eyckens DJ, Henderson LC (2019) Front. Chem. 7: 263.
Hallett JP, Welton T (2011) Chem. Rev. 111: 3508—3576.
Kaur G, Kumar H, Singla M (2022) J. Mol. Liq. 351: 118556.
Li AJ, Pal VK, Kannan K (2021) Environ. Chem. Ecotoxicol. 3: 91—116.
National Institute of Standards and Technology (2021) NIST Chemistry Webbook, US Department of Commerce, Washington, DC, USA.
Nieto de Castro CA, Langa E, Morais AL, Matos Lopes ML, Lourenço MJV, Santos FJV, Santos MSCS, Canongia Lopes JN, Veiga HIM, Macatrão M, Esperança JMSS, Marques CS, Rebelo LPN, Afonso CAM (2010) Fluid Phase Equilib. 294: 157—179.
Redlich O, Kister AT (1948) Ind. Eng. Chem. 40: 345—348.
Steltenpohl P, Graczová E (2022) Acta Chim. Slov. 15: 18—28.
Tariq M, Forte PAS, Costa Gomes MF, Conongia Lopes JN, Rebelo LPN (2009) J. Chem. Thermodyn. 41: 790—798.
Welton T (1999) Chem. Rev. 99: 2071—2084.
Wood SE, Battino R (1990) Thermodynamics of Chemical Systems. Cambridge University Press, Cambridge, UK.
Zhang QG, Cai SY, Zhang WB, Lan YL, Zhang XY (2017) J. Mol. Liq. 233: 471—478.